Received: 15 December 2021 | Accepted: 8 April 2022

DOI: 10.1002/hep4.1973

ORIGINAL ARTICLE

Gasdermin D–mediated pyroptosis suppresses liver regeneration after 70% partial hepatectomy

Xingyu Lv[1,2] | Jiang Chen[1,2] | Jiayan He[1,2] | Lidan Hou[1,2] | Yiyue Ren[1,2] | Xiaoyun Shen[2] | Yifan Wang[1,2] | Tong Ji[1,2] | Xiujun Cai[1,2]

[1]Department of General Surgery, Sir Run Run Shaw Hospital, Zhejiang University School of Medicine, Hangzhou, China

[2]Zhejiang Provincial Key Laboratory of Laparoscopic Technology, Hangzhou, China

Correspondence
Yifan Wang, Tong Ji and Xiujun Cai, Institute of Minimally Invasive Surgery, Sir Run Run Shaw Hospital, Zhejiang University School of Medicine, No. 3, Qingchun Road East, Hangzhou 310016, China.
Email: anwyf@163.com, jitong@zju.edu.cn and srrsh_cxj@zju.edu.cn

Funding information
Supported by the National Natural Science Foundation of China (81700551 and 81702854) and Key Research & Development Project in Zhejiang Province (2018C03083 and 2020C03122).

Abstract

Pyroptosis is a kind of programmed cell death primarily mediated by gasdermin D (GSDMD) and shown to regulate multiple diseases. However, its contribution to liver regeneration, a fine-tuned tissue repair process mediated primarily by hepatocytes after mass loss, remains unclear. Herein, we found that caspase-11/GSDMD-mediated pyroptosis was activated in regenerating liver after 70% partial hepatectomy. Impeding pyroptosis by deleting GSDMD significantly reduced liver injury and accelerated liver regeneration. Mechanistically, GSDMD deficiency up-regulates the activation of hepatocyte growth factor/c-Met and epidermal growth factor receptor mitogenic pathways at the initiation phase. Moreover, activin A and glypican 3 (GPC3), two terminators of liver regeneration, were inhibited when GSDMD was absent. *In vitro* study suggested the expressions of activin A and GPC3 were induced by interleukin (IL)–1β and IL-18, whose maturations were regulated by GSDMD-mediated pyroptosis. Similarly, pharmacologically inhibiting GSDMD recapitulates these phenomena. *Conclusion:* This study characterizes the role of GSDMD-mediated pyroptosis in liver regeneration and lays the foundation for enhancing liver restoration by targeting GSDMD in liver patients with impaired regenerative capacity.

INTRODUCTION

The liver is a unique organ with a high capacity for regeneration after mass loss.[1] There is strong evidence that liver parenchymal cells, hepatocytes, mediate liver regeneration under physiological and most pathological conditions.[2] Clinically, defective liver regeneration is associated with poor prognoses in many liver diseases, including chronic and acute hepatitis, transplantation, and liver cancer.[3] In rodents, a 70% partial hepatectomy (70%PH) is a paradigm for investigating liver regeneration. After surgery, nearly all hepatocytes re-enter the cell cycle and restore liver mass within 5–7 days in rats and mice.[4] The process of liver regeneration after 70%PH can be divided into three phases: initiation/priming, progression, and termination.[5] After decades of investigation, multiple cytokines, growth factors, and pathways involved in the regulation of liver regeneration have been identified.[1,6] However, further investigation of this process is necessary for the development of therapies to manage defective liver regeneration in patients undergoing liver resection and transplantation.

Pyroptosis is a type of programmed cell death mediated by inflammatory caspases.[7] The terminal executor

of this process was not evident until Shao discovered that gasdermin D (GSDMD) was the downstream effector of plasma membrane rupture in pyroptosis.[8] Following stimulus exposure, GSDMD is cleaved by caspase-1, caspase-4, and caspase-5 in humans or caspase-1 and caspase-11 in mice.[7] The 30-kDa N-terminal GSDMD subunits generate oligomers and form a ring-shaped pore on the plasma membrane. These GSDMD pores cause lytic, pro-inflammatory cell death and facilitate the release of interleukin (IL)–1β and IL-18.[9] In addition to GSDMD, more members of the gasdermin family with pore-formation ability were discovered.[10] By now, GSDMD-mediated pyroptosis has been reported to regulate multiple diseases.[11–14] However, the contribution of GSDMD-mediated pyroptosis on other biological processes, such as tissue homeostasis and regeneration, has not been studied sufficiently. Additionally, previous studies have suggested that apoptosis promotes the termination of liver regeneration,[15] and pyroptosis and necroptosis were thought to take part in this process also, but yet to be determined. Therefore, we evaluated the effect of GSDMD-mediated pyroptosis on liver regeneration using GSDMD knockout (*GSDMD*$^{-/-}$) mice in a classical 70%PH model, and the underlying mechanisms were explored. Additionally, the effect of the pharmacological inhibition of GSDMD on liver regeneration was examined to lay the foundation for potential clinical applications.

MATERIALS AND METHODS

Reagents

Disulfiram (DSF; HY-B0240), 5-bromo-2′-deoxyuridine (BrdU; HY-15910), caspase-11 inhibitor Wedelolactone (HY-N0551), and caspase-1 inhibitor Belnacasan (VX-765; HY-13205) were obtained from MedChemExpress. Recombinant mouse IL-1β (50101-MNAE) and IL-18 (50073-MNCE) were obtained from SinoBiological. Collagen type I (354236) was purchased from Corning. Collagenase IV (C5138) was obtained from Sigma-Aldrich.

Animal experiments

All animal experiments were performed according to the Institutional Animal Care and Use Committee guidelines of Zhejiang University, which are in accordance with the National Institutes of Health guidelines. Mice were housed in a pathogen-free facility under controlled temperature (22 ± 2°C) and lighting (12-hours light/dark cycle) conditions. The mice were given regular food and autoclaved water.

The *GSDMD*$^{-/-}$ mice with a C57BL/6 background were obtained from Pro Chong Liu in Navy Military Medical University. Eight-week-old to 10-week-old male C57BL/6 wild-type mice were purchased from ZhiYuan. For DSF treatment, mice received intraperitoneal DSF (50 mg/kg) dissolved in sesame oil (10 mg/ml) or a vehicle (control), both 24 hours and 4 hours before surgery. For VX-765 treatment, mice (male, 8–10 weeks old) were treated with VX-765 (100 mg/kg) dissolved in sesame oil or a vehicle via oral gavage 4 hours before 70%PH. For Wedelolactone treatment, mice (male, 8–10 weeks old) received intraperitoneal Wedelolactone (10 mg/kg) dissolved in sesame oil or a vehicle 4 hours before 70%PH.

70% partial hepatectomy

A 70% PH was performed according to a previous report.[16] Briefly, mice were anesthetized with isoflurane, and the median and left lateral liver lobes were resected using sutures and ligation. The abdomen was then stitched using two-layer sutures. Remnant livers were collected at various times after 70%PH. A sham surgery without liver lobe resection was performed. For experiments of short time courses, samples of the sham group were collected at 1 hours after sham surgery. For experiments of long-term courses, samples of the sham group were collected at 48 hours after sham surgery. The amount of liver regeneration was determined by measuring the body and liver weights and calculating the liver/body ratio. For BrdU labeling, operated mice received intraperitoneal BrdU (100 mg/kg) 1 hours before being killed.

Immunohistochemistry

Liver tissues were fixed in 4% paraformaldehyde overnight, dehydrated in a graded alcohol series, and embedded in paraffin. Paraffin-embedded liver samples were cut into 3.5-μM-thick slides. Immunohistochemical staining for BrdU (MAB3262B; Millipore; 1:200) and phosphorylated histone H3 (p-H3; 9701; CST, 1:100) was performed using a DAB detection kit (GK600710; Gene company) according to the manufacturer's instructions. To count BrdU-positive and p-H3-positive hepatocytes, 10 random ×400 fields were calculated per slide from at least three mice from each group. The results are represented as means, with error bars indicating the SD.

Quantitative reverse-transcription polymerase chain reaction

Trizol was used for extracting RNA from the liver tissues. Complementary DNA was synthesized using the Hifair II 1st Strand cDNA Synthesis kit (Yeasen; 11119ES60), and gene expression was quantified using

the Hieff UNICON qPCR SYBR Green Master Mix kit (Yeasen; 11198ES03) according to the manufacturer's instructions. Gene expression was normalized to that of the housekeeping gene, GAPDH. The primers are listed in Table S1.

Western blotting

Liver tissues were homogenized in radio immunoprecipitation assay buffer containing proteinase and phosphatase inhibitors. After 30 min of incubation on ice, the samples were centrifuged for 15 min at 13,000 rpm at 4°C. The supernatants were collected, and a BCA kit (Thermo Fisher Scientific) was used for quantitation. Aliquots of liver protein lysate were subjected to sodium dodecyl sulfate polyacrylamide gel electrophoresis and then transferred onto polyvinylidenefluoride membranes. After blocking with 5% skimmed milk, the membrane was incubated with primary antibodies overnight. Subsequently, the membranes were incubated with horseradish peroxidase–conjugated secondary antibodies for 1 hours. Protein bands were visualized using the electrogenerated chemiluminescence reaction. The antibodies are listed in Table S2.

Hepatocyte perfusion

Hepatocyte perfusion was performed as previous reported.[17] Briefly, the abdomen of anesthetized mouse was opened after swabbing with 70% ethanol. Then, liver was perfused through inferior vena caca with consecutive buffer A (buffer B with 0.5 mM ethylene glycol tetraacetic acid), buffer B (30 ml KCl, 1.3 M NaCl, 10 mM NaH_2PO_4, 100 mM glucose, and 100 mM 4-(2-hydroxyethyl)-1-piperazine ethanesulfonic acid), and buffer C (buffer B with 5 mM $CaCl_2$ and 30 mg collagenase IV). Digested liver was suspended in 50 ml of sterilized phosphate-buffered saline (PBS) and passed through a 100-μM nylon mesh. Subsequently, filtered PBS with cells were centrifugated at 50*g* for 5 min at 4°C, and the pelleted cells were hepatocytes. For planting hepatocytes, dishes were covered with collagen type I with concentration of 50 ug/ml for 1 hours at room temperature, which was dissolved in 0.2 M acetic acid solution.

Cell experiments

The alpha mouse liver 12 (AML12) cell line was purchased from the Cell Bank of the Chinese Academy of Sciences (Shanghai, China) and cultured in Dulbecco's modified Eagle's medium (DMEM) supplemented with 10% fetal bovine serum (FBS) and antibiotics. Cells were maintained in a humidified incubator with 5% CO_2 at 37°C. For IL-1β treatment, AML12 cells and primary mouse hepatocytes were cultured in 0.2% FBS-DMEM 24 hours before IL-1β was added, after which the indicated dose of IL-1β was added to the 0.2% FBS-DMEM and the cells were incubated for another 6 hours. For IL-18 treatment, indicated final concentration of IL-18 was added to the medium and incubated for 48 hours.

Serum alanine aminotransferase measurement

Blood samples were collected for serum preparation. Alanine aminotransferase (ALT) activity was detected using an ALT assay kit according to the manufacturer's instructions (Nanjing Jiancheng).

Enzyme-linked immunosorbent assay

Blood samples were collected for serum preparation. The levels of serum IL-18, IL-1β, IL-6, and tumor necrosis factor α (TNFα) were measured with enzyme-linked immunosorbent assay (ELISA) kits according to the manufacturer's instructions (MULTI SCIENCES).

Statistical analysis

GraphPad Prism VII software was used for the statistical analyses. The Student's *t* test was used for data analysis, and results are presented as the mean ± SD. *p* value < 0.05 was considered statistically significantly.

RESULTS

GSDMD cleaved by CASPASE-11 is detected in liver regeneration after 70%PH

To determine whether pyroptosis was activated during liver regeneration, GSDMD expression and cleavage were detected. A 70%PH was performed on wild-type mice, and liver samples were harvested at various time points for quantitative polymerase chain reaction (PCR) and western blotting. Although the messenger RNA (mRNA) levels did not vary much (Figure 1A), truncations of GSDMD, caspase-1, and caspase-11 were easily detected at all indicated time points following operation (Figure 1B,C). Next, wild-type mice were divided into four groups and treated with oil, caspase-1 inhibitor VX-765, caspase-11 inhibitor Wedelolactone, and combination of VX-765 and Wedelolactone separately. Liver samples with different treatments were harvested at 48 hours after 70%PH to analyze the truncation of GSDMD. As shown in Figure 1D,E, cleavage of GSDMD was abolished in the presence of Wed,

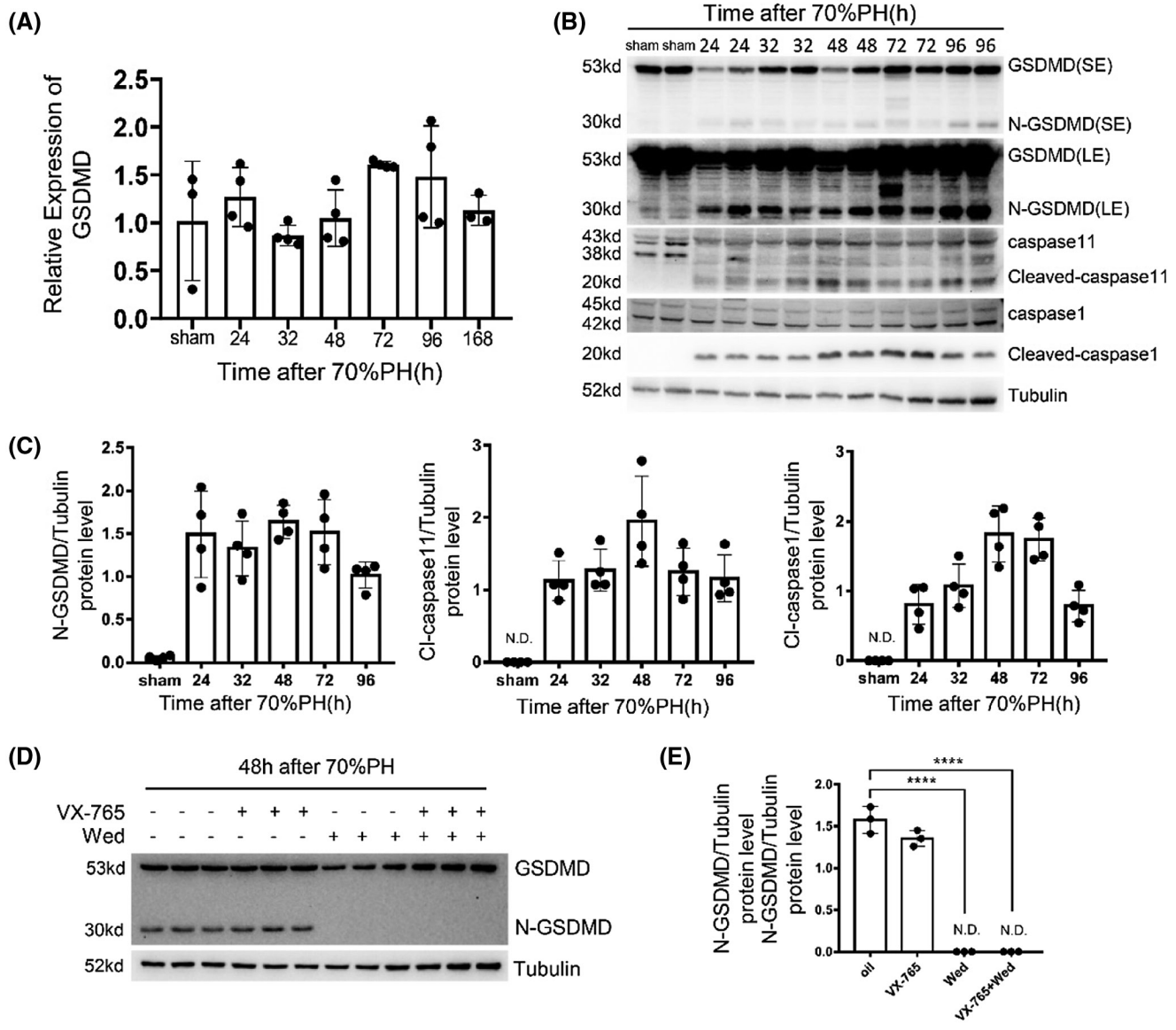

FIGURE 1 Detecting liver regeneration and injury in gasdermin D (GSDMD) knockout and wild-type mouse after 70% partial hepatectomy (70%PH). (A) The messenger RNA (mRNA) level of GSDMD at indicated time points after 70%PH was measured by quantitative polymerase chain reaction (PCR; n = 3–4/group). (B) The cleavage of caspase-1, caspase-11, and GSDMD in remnant livers after 70%PH was measured by western blotting. Tubulin served as loading controls. (C) Quantification of western blotting results in (B). (D) Protein levels of GSDMD and its N terminus in livers of mice treated with oil, Belnacasan (VX-765), Wed, and combination of VX-765 and Wed at 48 hours after 70%PH were measured by western blotting. (E) Quantification of western blotting results found in (D). The sham group sample was collected at 48 hours after sham surgery. Data are presented as mean ± SD; ****$p < 0.0001$. LE, long exposure; N.D., not detected; SE, short exposure

while no effect of VX-765 was found on this processing. Thus, cleavage of GSDMD was activated in regenerating livers after 70%PH, which was mediated by caspase-11.

GSDMD deficiency accelerates liver regeneration after 70%PH

To explore the role of GSDMD-mediated pyroptosis in liver regeneration, GSDMD knockout (*GSDMD*$^{-/-}$) mice were used. An illustration of GSDMD$^{-/-}$ mice and genotyping results is shown in Figure S1A,B, and western blotting confirmed vanish of GSDMD in knockout mice (Figure S1C). Moreover, GSDMD heterozygous mice showed an equivalent level of GSDMD with wild-type mice. Next, adult GSDMD wild-type, heterozygous, and knockout mice were subjected to surgery, and liver regeneration was analyzed. Accelerated liver regeneration, measured by the liver/body weight ratio, was observed in *GSDMD*$^{-/-}$ mice compared with controls at 72 hours and 96 hours after operation (Figure 2A). Liver injury was attenuated by deleting GSDMD, as reflected by serum ALT levels (Figure 2B). DNA replication and

mitosis of hepatocytes were measured by immunohistochemistry for BrdU and p-H3 on liver slides. Consistent with the suggestion of accelerated liver regeneration in *GSDMD*$^{-/-}$ mice, there were significantly more BrdU-positive and p-H3-positive hepatocytes detected in the regenerating livers of *GSDMD*$^{-/-}$ mice at 48 hours and 72 hours after operation compared with *GSDMD*$^{+/+or-}$ mice (Figure 2C,D), which was confirmed by western blotting for proliferating cell nuclear antigen and p-H3 (Figure 2E). On quantitative PCR, the mRNA level of cyclin D1 was found to have significantly increased in the livers of knockout mice at 48 hours and 72 hours after 70%PH. The elevated expression of cyclin E1 in *GSDMD*$^{-/-}$ mice was also observed at 24 hours postoperatively (Figure 2F). Taken together, these results suggest that the removal of GSDMD attenuates liver injury postoperatively and accelerates liver regeneration at 48 hours and 72 hours after 70%PH.

Removing GSDMD up-regulates mitogenic signaling pathways at the initiation stage of liver regeneration

To determine whether GSDMD modulates the initiation of liver regeneration, samples were collected at 1, 2, and 4 hours after 70%PH. In terms of liver injury, *GSDMD*$^{-/-}$ mice had significantly attenuated damage at all three time points following operation (Figure 3A), and cleaved GSDMD was also easily detected after surgery. Both truncation of caspase-1 and caspase-11 was evident at 1, 2, and 4 hours after operation (Figure 3B,C).

Multiple genes and mitogen signaling pathways were activated immediately following the 70%PH, including the epidermal growth factor receptor (EGFR)/hepatocyte growth factor (HGF)/hedgehog/tumor necrosis factor receptor-1 pathway and the yes-associated protein/β-catenin/nuclear factor κB pathway.[15] A series of western blotting analyses were conducted to clarify the effect of the removal of GSDMD on this process. As shown in Figure 4A, the EGFR signaling pathway was significantly elevated in *GSDMD*$^{-/-}$ mice, as demonstrated by the increase in phosphorylated EGFR (p-EGFR) and downstream phosphorylated mammalian target of rapamycin/phosphorylated Akt/phosphorylated extracellular signal–regulated kinase/phosphorylated signal transducer and activator of transcription-3 (p-STAT3) pathway at 1, 2, and 4 hours postoperatively. The HGF/c-Met pathway was also up-regulated in the livers of *GSDMD*$^{-/-}$ mice at 4 hours after surgery, as indicated by increased level of p-c-Met. The expressions of EGFR ligands (transforming growth factor α [TGFα], heparin-binding epidermal growth factor, and amphiregulin) and the c-Met ligand (HGF) were measured by quantitative PCR. As shown in Figure 4B, significantly elevated expressions of amphiregulin and heparin-binding epidermal growth factor were detected as early as 1 hours and 4 hours after surgery, respectively, in *GSDMD*$^{-/-}$ mice compared with controls. HGF expression was significantly increased in the livers of *GSDMD*$^{-/-}$ mice at 4 hours postoperatively. In addition, the mRNA level of smooth muscle actin (SMA), a biomarker of activated hepatic stellate cells secreting HGF to promote liver regeneration, was also significantly increased at 4 hours postoperatively. Macrophages are important for initiating liver regeneration after 70%PH by secreting IL-6 and TNFα. However, macrophage content was not changed by deleting GSDMD, reflected by quantitative PCR for F4/80 (Figure S2A). Western blotting and ELISA also showed equivalent amount of IL-6 and TNFα between GSDMD wild-type and knockout mice (Figure 4A and Figure S2B). Taken together, these data suggest that GSDMD-mediated pyroptosis inhibits the activation of the mitogenic HGF/c-Met and the EGFR signaling pathways in the initiation phase of liver regeneration, partly by reducing the expression of amphiregulin and HGF.

GSDMD regulates the termination of liver regeneration via IL-18/GLYPICAN-3 axis

Mitogenic pathways were upregulated in *GSDMD*$^{-/-}$ mice at the initiation phase, whereas this phenomenon was not observed at 48 hours and 72 hours after 70%PH (Figure S4A). We considered that IL-18, a pro-inflammatory cytokine whose secretion is facilitated by N-GSDMD pores, has been reported to promote the termination of liver regeneration by up-regulating glypican 3 (GPC3).[18] To determine whether this mechanism accelerated liver regeneration in *GSDMD*$^{-/-}$ mice, the levels of GPC3 and pro and mature IL-18 were examined. No significant difference in IL-18 expression between *GSDMD*$^{-/-}$ and control mice was found on quantitative PCR; however, the mRNA and protein levels of GPC3 significantly decreased in the livers of GSDMD knockout mice at indicated time points after surgery (Figure 5A,B). Although the mRNA expression of IL-18 was not changed, the level of serum IL-18 of *GSDMD*$^{-/-}$ mice was significantly reduced at 48 hours and 72 hours after operation (Figure 5C), and maturation of IL-18 in liver tissues reflected by cleaved IL-18 was also decreased at 48 hours and 72 hours after surgery (Figure S3A). To explore whether IL-18 promotes GPC3 expression in hepatocytes directly, purified primary hepatocytes from wild-type mice were treated with the indicated concentration of IL-18 for 48 hours. As shown in Figure 5D, the mRNA and protein levels of GPC3 in primary hepatocytes were significantly increased after IL-18 treatment. These findings suggest that GSDMD-mediated pyroptosis promotes the maturation of IL-18, which promotes GPC3 expression in hepatocytes to suppress liver regeneration.

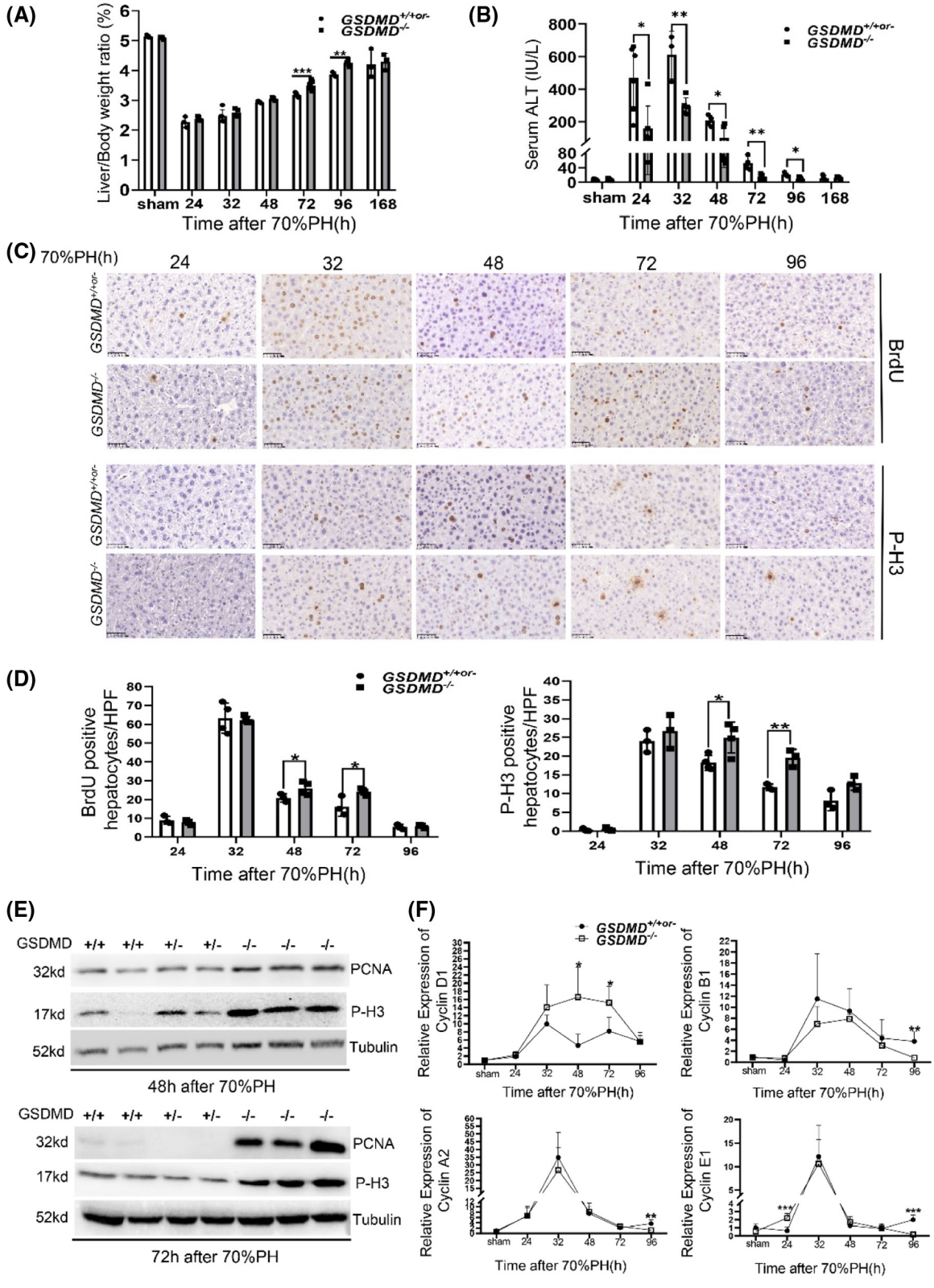

Elevated expression of activin a mediated by IL-1β is another downstream of GSDMD to terminate liver regeneration

Activin A is a well-known repressor of liver regeneration, which terminates liver regeneration through phosphorylating mothers against decapentaplegic homolog 2 (smad2).[19] Intriguingly, its expression was found to be significantly decreased in *GSDMD*$^{-/-}$ mice at 48 hours and 72 hours after operation (Figure 6A). A previous study showed that IL-1β promotes the expression of activin A in skin fibroblasts,[20] and serum IL-1β

FIGURE 2 GSDMD deficiency enhanced the proliferation of hepatocytes after 70%PH. Liver regeneration and injury between $GSDMD^{+/+or-}$ and $GSDMD^{-/-}$ mice at various time points after 70%PH were evaluated by liver/body weight ratio (A) and serum alanine aminotransferase (ALT) (B) ($GSDMD^{+/+}$, n = 3/group; $GSDMD^{+/-}$, n = 0–2/group; $GSDMD^{-/-}$, n = 3–8/group). (C) Representative pictures of immunohistochemistry (IHC) for 5-bromo-2′-deoxyuridine (BrdU) and phosphorylated histone H3 (p-H3) in liver slides at indicated time points after surgery; ×400; scale bars, 50 μM. (D) Quantification of positive hepatocytes shown in (C) ($GSDMD^{+/+}$, n = 3/group; $GSDMD^{+/-}$, n = 0–1/group; $GSDMD^{-/-}$, n = 3–4/group); graphs represent mean ± SD of $BrdU^+$ and $p\text{-}H3^+$ hepatocytes/high-power field (HFP). (E) Western blotting for proliferating cell nuclear antigen (PCNA) and p-H3 at 48 hours and 72 hours after surgery. Tubulin served as loading controls. (F) Quantitative PCR for cyclin D1, cyclin A2, cyclin B1, and cyclin E1 in liver tissues from $GSDMD^{+/+or-}$ and $GSDMD^{-/-}$ mice at various time points after 70%PH ($GSDMD^{+/+}$; n = 4/group; $GSDMD^{+/-}$, n = 0–3/group; $GSDMD^{-/-}$, n = 3–8/group). The sham group were collected at 48 hours after sham surgery. Data are presented as mean ± SD; $*p < 0.05$, $**p < 0.01$, $***p < 0.001$

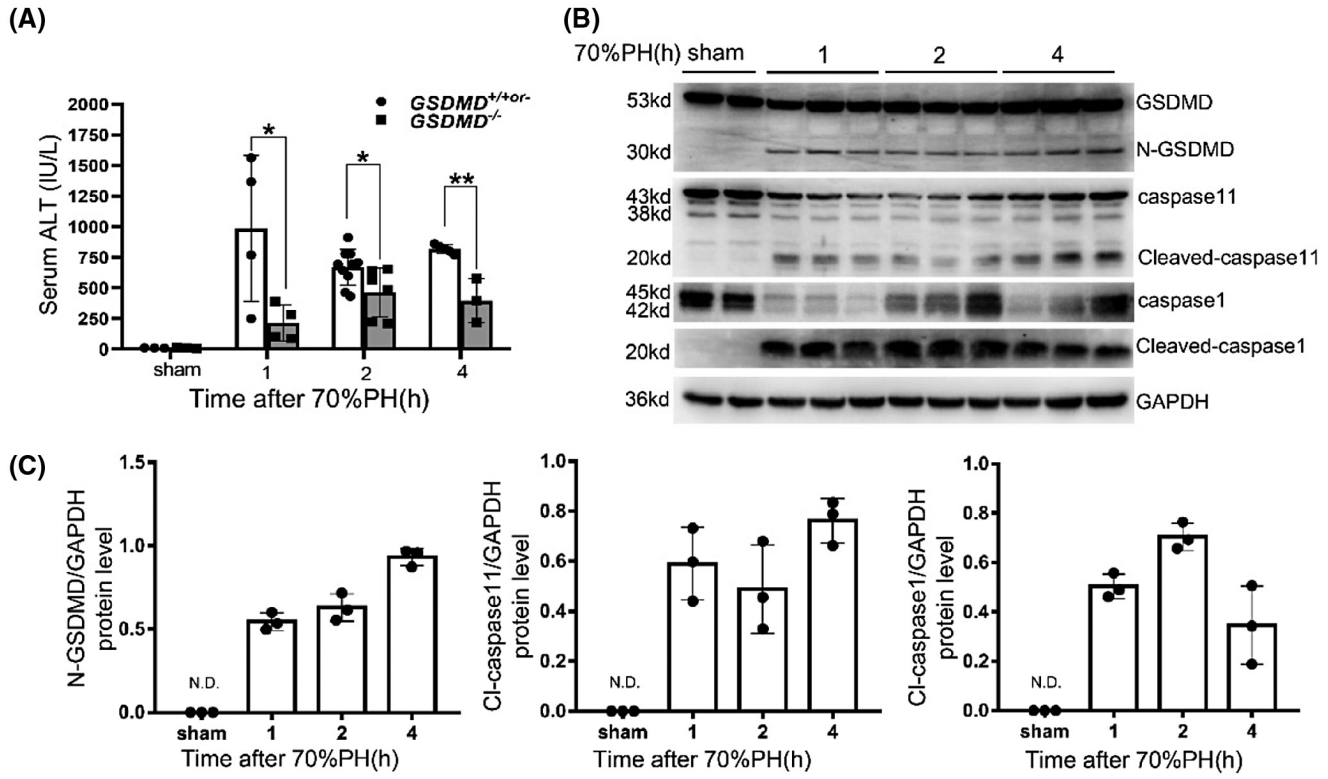

FIGURE 3 Attenuation of liver injury at initiation phase of liver regeneration by deleting GSDMD. (A) Serum ALT activity was measured to evaluate liver injury ($GSDMD^{+/+}$, n = 3–5/group; $GSDMD^{+/-}$, n = 0–4/group; $GSDMD^{-/-}$, n = 3–9/group). (B) Western blotting for cleavage of caspase-1, caspase-11, and GSDMD at indicated time points after 70%PH. Glyceraldehyde 3-phosphate dehydrogenase (GAPDH) served as loading controls. (C) Quantification of western blotting results found in (B). The sham group were collected at 1 hours after sham surgery. Data are presented as mean ± SD; $*p < 0.05$, $**p < 0.01$

was significantly reduced in $GSDMD^{-/-}$ mice concurrently (Figure 6B). The protein levels of activin A, its downstream smad2/3, and pro and mature IL-1β were detected by western blotting. As shown in Figure 6C, significantly reduced activin A and phosphorylated smad2 (p-smad2) were detected in $GSDMD^{-/-}$ mice. Maturation of IL-1β reflected by cleaved IL-1β was also decreased by deleting GSDMD. Moreover, TGFβ, another upstream of p-smad2, did not vary much between $GSDMD^{+/+or-}$ and $GSDMD^{-/-}$ mice, further supporting the involvement of activin A/smad2 axis in the termination of liver regeneration mediated by GSDMD.

To ascertain, elevated expression of activin A was induced by IL-1β in hepatocytes. The AML12 cell line and primary hepatocytes purified from wild-type mice were treated with IL-1β at indicated concentration for 6 hours. Then the expression of activin A was analyzed. As shown in Figure 6D,E, the mRNA and protein levels of activin A were significantly increased after IL-1β treatment in both tested cells. The effect of IL-1β treatment was verified by prostaglandin endoperoxide synthase, a well-known target of IL-1β. Collectively, these findings suggested that the IL-1β/activin A/smad2 pathway is another downstream regulator of liver regeneration mediated by GSDMD.

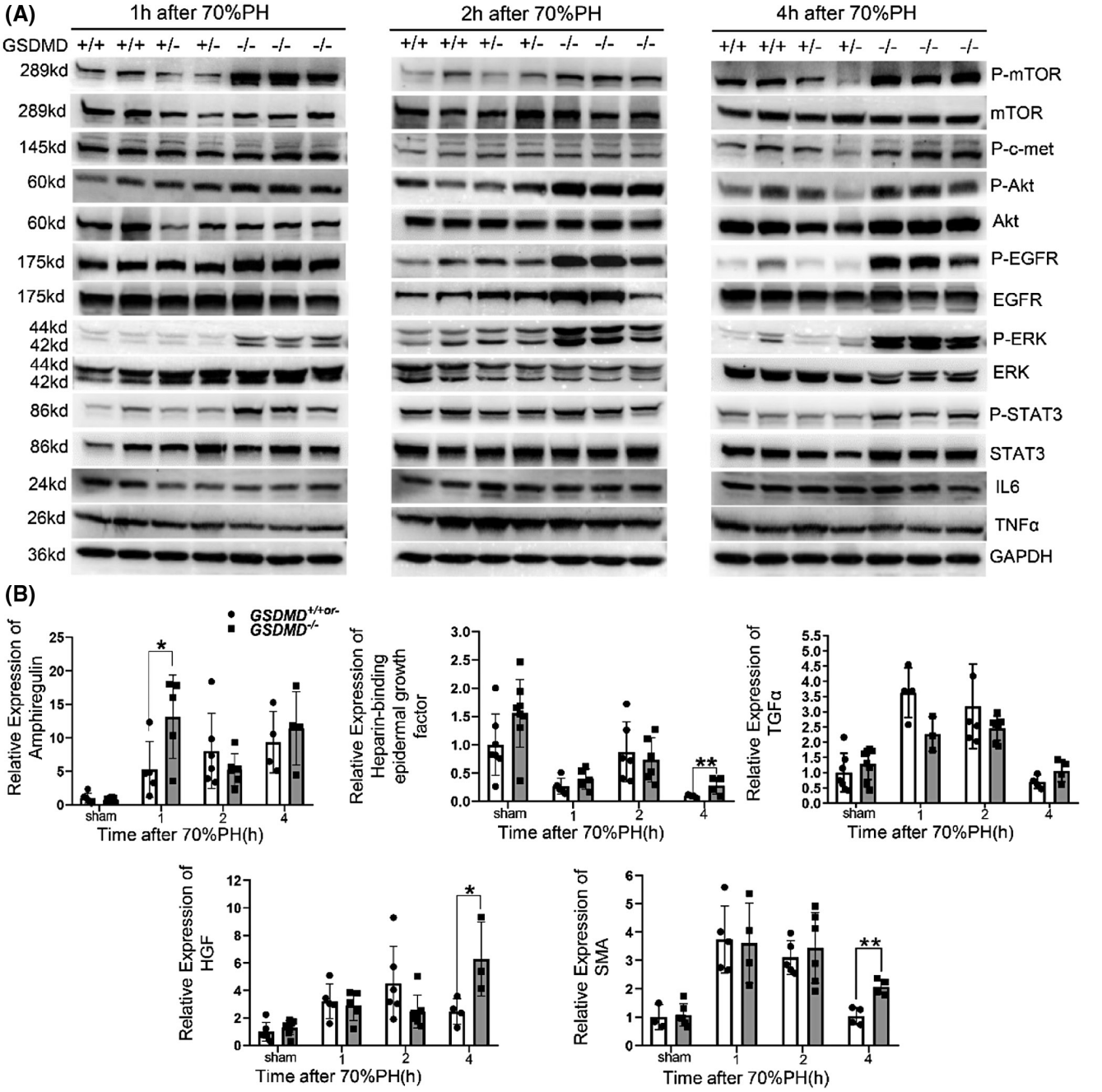

FIGURE 4 Deletion of GSDMD attenuated the activation of hepatocyte growth factor (HGF)/c-Met–mediated and epidermal growth factor receptor (EGFR)–mediated mitogenic pathways at initiation phase of liver regeneration. (A) Examining the activation of HGF/c-Met and EGFR signaling pathway by western blotting for phosphorylated c-Met (p-c-Met), phosphorylated EGFR (p-EGFR)/EGFR, phosphorylated extracellular signal–regulated kinase (p-ERK)/ERK, phosphorylated Akt (p-Akt)/Akt, and phosphorylated signal transducer and activator of transcription-3 (p-STAT3)/STAT3 at indicated time points after 70%PH. GAPDH served as loading controls. (B) Quantitative PCR for measuring the mRNA levels of HGF and EGFR ligands Amphiregulin (Areg), Heparin-binding epidermal growth factor (HB-EGF), and transforming growth factor α (TGFα) in remnant livers of $GSDMD^{+/+or-}$ and $GSDMD^{-/-}$ mice ($GSDMD^{+/+}$, n = 3–5/group; $GSDMD^{+/-}$, n = 0–3/group; $GSDMD^{-/-}$, n = 3–8/group). The sham group were collected at 1 hours after sham surgery. Data are presented as mean ± SD; $*p < 0.05$, $**p < 0.01$. IL, interleukin; mTOR, mammalian target of rapamycin; TNFα, tumor necrosis factor α

GSDMD inhibitor disulfiram accelerates liver regeneration after 70%PH

DSF is a Food and Drug Administration–approved drug for the treatment of alcoholism. A recent study found that DSF can also block the pore-forming function of GSDMD.[21] Thus, DSF was injected into wild-type mice to determine whether pharmacological inhibition of GSDMD could mimic the phenotype observed in $GSDMD^{-/-}$ mice. As shown in Figure 7A,

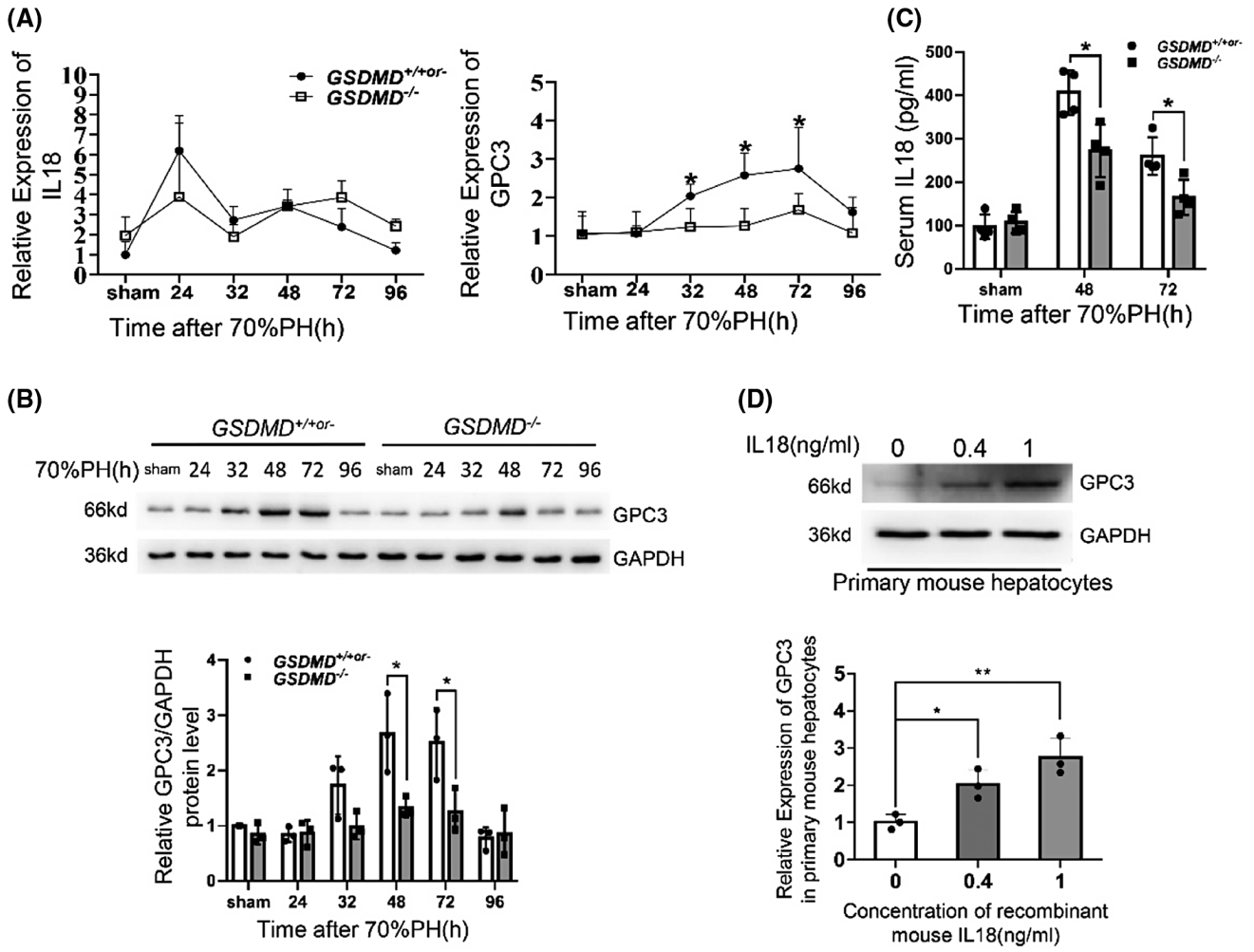

FIGURE 5 Attenuation of IL-18/glypican 3 (GPC3) axis in livers of *GSDMD*$^{-/-}$ mice compared with controls after surgery. (A) The mRNA levels of IL-18 and GPC3 were measured by quantitative PCR (*GSDMD*$^{+/+}$, n = 3–5/group; *GSDMD*$^{+/-}$, n = 0–3/group; *GSDMD*$^{-/-}$, n = 3–8/group). (B) Western blotting for GPC3 in remnant livers of *GSDMD*$^{+/+or-}$ and *GSDMD*$^{-/-}$ mice at various time points after 70%PH. GAPDH served as loading control. (C) Serum IL-18 was detected by enzyme-linked immunosorbent assay (ELISA; *GSDMD*$^{+/+}$, n = 3/group; *GSDMD*$^{+/-}$, n = 1/group; *GSDMD*$^{-/-}$, n = 4/group). (D) Primary mouse hepatocytes were treated with indicated concentration of recombinant IL-18 for 48 hours, and the mRNA and protein levels of GPC3 were analyzed by quantitative PCR and western blotting. The sham group were collected at 48 hours after sham surgery. Data are presented as mean ± SD; $*p < 0.05$, $**p < 0.01$

the liver/body weight ratio clearly increased in DSF-treated mice at 48 hours and 72 hours after surgery, accompanied by reduced liver injury. Proliferation of hepatocytes evaluated by immunohistochemistry for BrdU and p-H3 showed a significant increment in S-phase and M-phase hepatocytes after DSF treatment (Figure 7B,C). ELISA showed the levels of serum IL-1β and IL-18 were significantly reduced by DSF treatment (Figure 7D). We also detected changes in IL-18/GPC3 and the IL-1β/activin A/smad2 axis, consistent with the findings in *GSDMD*$^{-/-}$ mice. These two pathways were also down-regulated in mice subjected to DSF (Figure 7E). Collectively, these data suggested that pharmacological inhibition of GSDMD by DSF accelerates liver regeneration after 70%PH, as observed in *GSDMD*$^{-/-}$ mice.

DISCUSSION

Previous studies about GSDMD focused primarily on pathophysiological processes. In this study, we demonstrated that GSDMD-mediated pyroptosis modulates liver regeneration, a tissue repair process. Mechanistically, GSDMD neutralizes mitogenic pathways required for the initiation phase of liver regeneration and terminates liver regeneration by secreting IL-1β and IL-18.

Different from apoptotic reaction, which primarily occurs at the termination phase of liver regeneration,[22] GSDMD-mediated pyroptosis was detected at a much broader time course, ranging from initiation to termination phase. Deleting GSDMD also significantly reduced liver injury at certain time points following operation. Hence, it

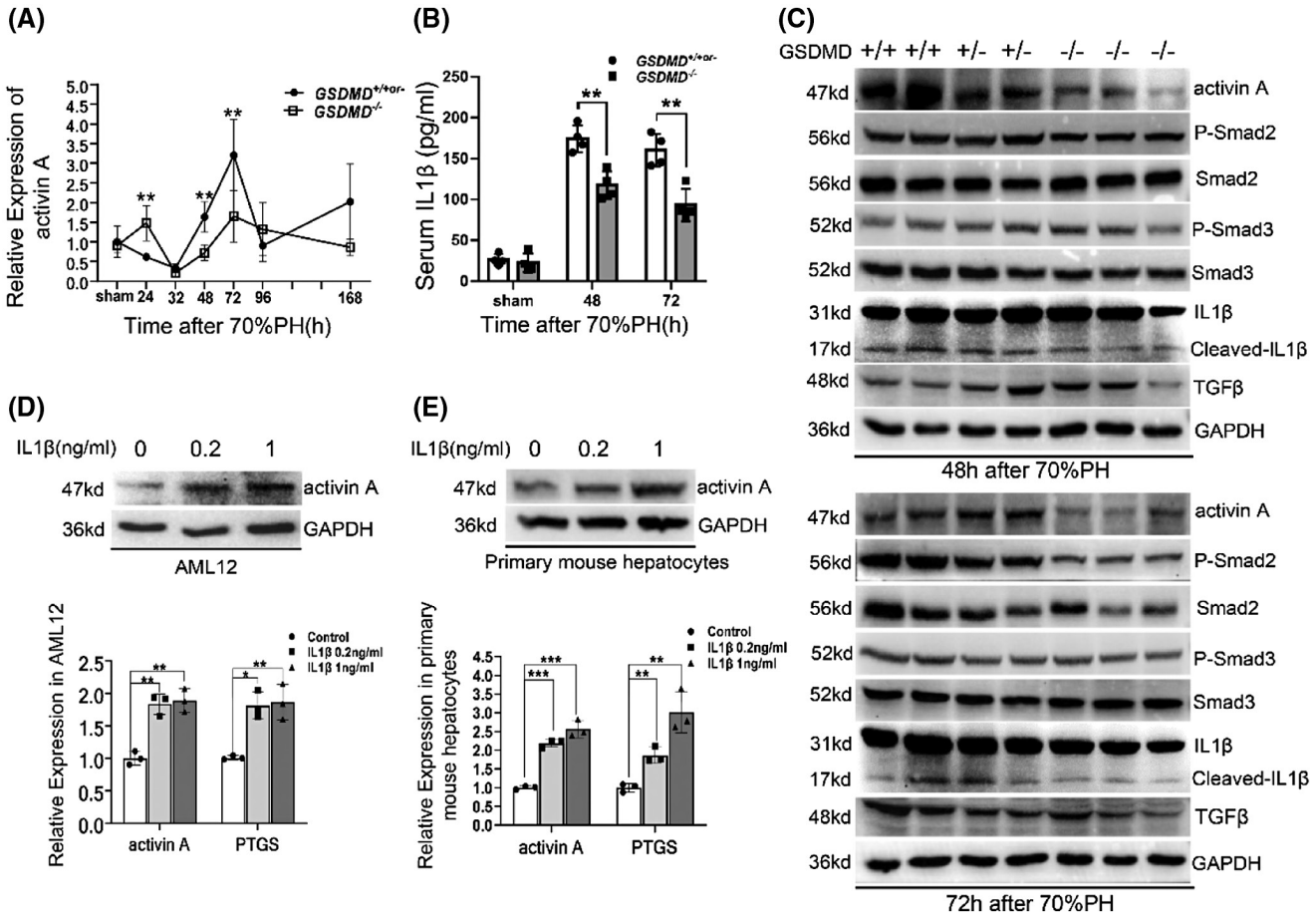

FIGURE 6 IL-1β-induced expression of activin A in hepatocyte was blocked in *GSDMD*$^{-/-}$ mice. (A) Quantitative PCR for the mRNA level of activin A at various time points after 70%PH (*GSDMD*$^{+/+}$, n = 4/group; *GSDMD*$^{+/-}$, n = 0–4/group; *GSDMD*$^{-/-}$, n = 4–8/group). (B) Serum IL-1β was detected by ELISA (*GSDMD*$^{+/+}$, n = 3/group; *GSDMD*$^{+/-}$, n = 1/group; *GSDMD*$^{-/-}$, n = 4/group). (C) The protein level of activin A and activation of mothers against decapentaplegic homolog (smad) 2, smad3, and IL-1β were examined by western blotting at 48 hours and 72 hours after 70%PH. (D,E) Alpha mouse liver 12 (AML12) cell line (D) and primary mouse hepatocytes (E) were treated with indicated dose of mature IL-1β for 6 hours, then the protein level of activin A and mRNA levels of activin A and prostaglandin endoperoxide synthase (PTGS) were measured by quantitative PCR and western blotting. GAPDH served as loading controls of western blotting. Cell experiments were performed 3 times and are presented as the mean ± SD; $*p < 0.05$, $**p < 0.01$. The sham group were collected at 48 hours after sham surgery. p-Smad, phosphorylated Smad

is reasonable that GSDMD-mediated pyroptosis is one of the major reasons for liver injury after liver resection, and it exerts more functions than apoptosis, not only terminating liver regeneration, but also increasing liver damage. GSDMD could be cleaved by caspase-1, caspase-4, caspase-5 and caspase-11, known as the canonical and non-canonical pathways, respectively. In addition, recent studies suggested that TGF-β activated kinase-1 inhibition triggered caspase-8-dependent cleavage of GSDMD, and elastase mediated GSDMD processing in aging neutrophil.[23] The contribution of GSDMD processing mediated by different upstream caspases on pathological process has been elucidated in various diseases, such as alcohol-associated hepatitis, acute kidney injury, and sepsis.[12,13,24] Distinct from caspase-1, whose activation was mediated by NOD-, LRR- and pyrin domain-containing protein 3 inflammasome, caspase-11 could be activated by direct interaction with oxidized phospholipids or lipopolysaccharides (LPS),[23] a component of gram-negative bacteria. Presently, abolishment of truncated GSDMD by caspase-11 inhibitor Wed had no effect on caspase-1 inhibitor VX-765, suggesting that GSDMD-mediated pyroptosis was induced by a noncanonical pathway after 70%PH. Considering the fact that remnant liver was exposed to increased level of gut-derived LPS after 70%PH,[25] it could be concluded that capase11 is the upstream caspase responsible for GSDMD processing during liver regeneration.

HGF/c-Met-mediated and EGFR-mediated signaling pathways were activated as early as 30 min after surgery and are required for the initiation phase of liver regeneration.[26] Previous studies have demonstrated that blocking either of these pathways delays liver regeneration, while blocking both of them totally abrogates liver regeneration.[27–29] Presently, we found that the deletion of GSDMD increased the activation of the HGF/c-Met-mediated and EGFR-mediated pathways hours postoperatively. The up-regulation of these pathways could be

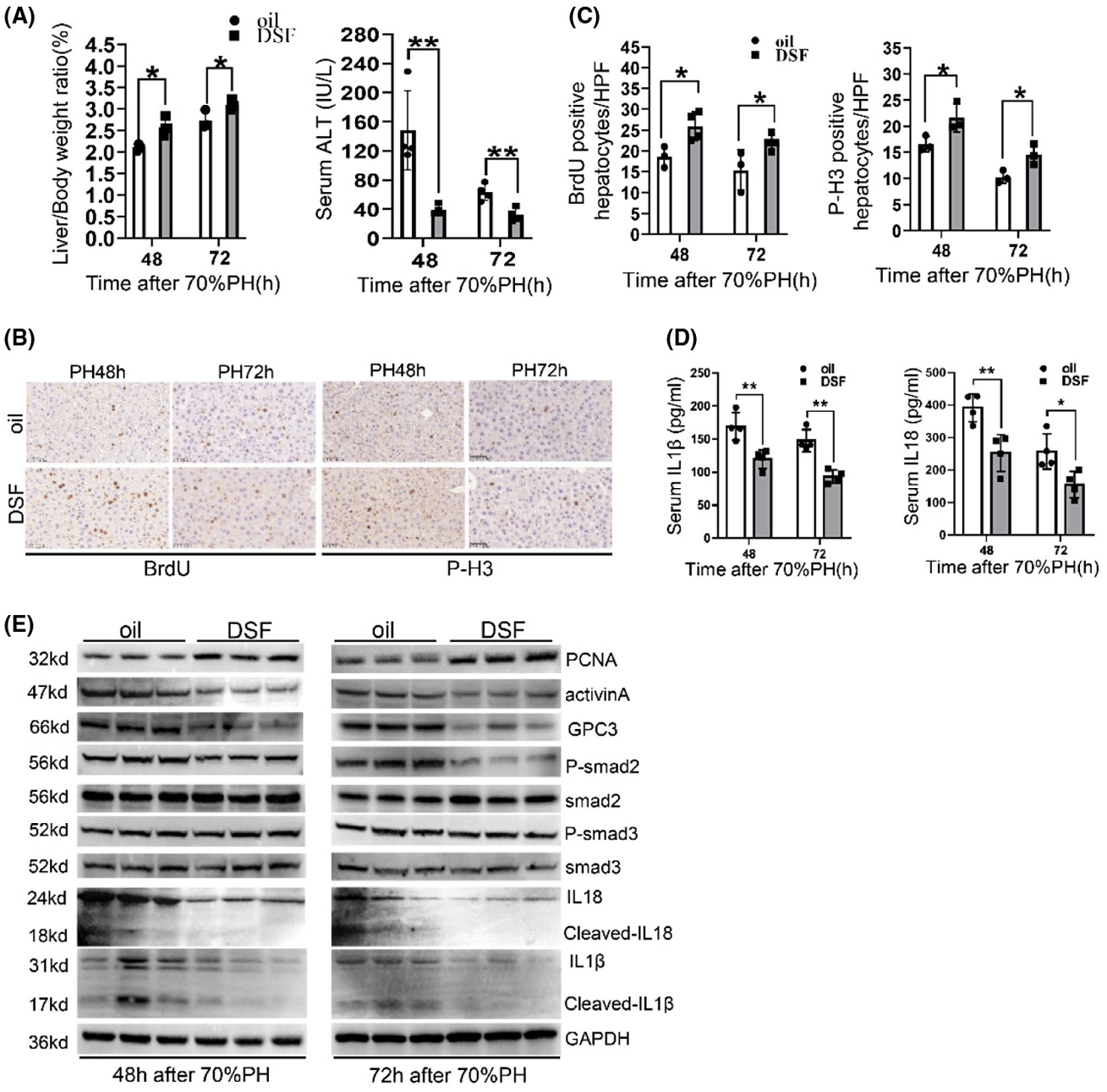

FIGURE 7 Pharmacological inhibition of GSDMD by DSF-ameliorated liver injury and regeneration after 70%PH. (A) Evaluating the degree of liver regeneration and liver injury in oil-treated and DSF-treated mice by measuring liver/body ratio and serum ALT. (B,C) Representative pictures and quantification for BrdU-positive and p-H3-positive hepatocytes in liver slides of oil-treated and DSF-treated mice at 48 hours and 72 hours after surgery (n = 3–4/group). (D) Serum IL-1β and IL-18 were detected by ELISA (n = 4/group). (E) The protein levels of PCNA, activin A, and activation of smad2/3, IL-1β, and IL-18 were examined by western blotting. GAPDH served as loading controls. Graphs represent mean ± SD of BrdU+ and p-H3+ hepatocytes/HFP. Data are presented as mean ± SD; $*p < 0.05$, $**p < 0.01$

attributed to the increased expression of amphiregulin and HGF, the ligands of EGFR and c-Met, respectively. It has been reported that amphiregulin and HGF are produced primarily by hepatocytes and activated stellate cells, respectively, in the liver.[30,31] Considering the decrement of liver injury and increment of the activated stellate cell marker SMA in *GSDMD*$^{-/-}$ mice, we speculated that more cells, including hepatocytes and stellate cells, would survive pyroptosis in the context of GSDMD deficiency, which up-regulates the expression of ligands responsible for mitogenic pathway activation.

Macrophage is required for initiating liver regeneration,[1] and its pyroptosis in canonical and noncanonical pathways has been reported.[32] However, deletion of GSDMD did not change macrophage content hours after operation, reflected by quantitative PCR for F4/80. Consistently, IL-6 and TNFα, two cytokines primarily secreted by macrophages, also did not vary much in

GSDMD deficiency. Thus, the increment of p-STAT3, a well-known downstream effector of IL-6, may be induced by EGFR signaling, which can also activate STAT3 by phosphorylation.[33]

It is well known that pores formed by N-GSDMDs facilitate the release of mature IL-1β and IL-18. In noncanonical pathway, the pores induced by the caspase-11/GSDMD cascade trigger an efflux of K^+, ultimately mediating cleavage of caspase-1 and subsequent maturation of IL-1β and IL-18.[34] IL-1β and IL-18 are two pleiotropic cytokines that mediate multiple pathological and physiological processes, including liver regeneration after 70%PH.[18,35,36] An earlier study performed in rats showed that IL-18 accelerates liver regeneration,[36] whereas a recent study using *IL-18*$^{-/-}$ mice suggested that it acts as an inhibitor of liver regeneration after 70%PH by up-regulating GPC3.[37] Herein, reduced maturation of IL-18 and decreased GPC3 expression were detected when GSDMD was absent. Therefore, consistent with the latter study, we believe that GPC3 expression in hepatocytes induced by IL-18 occurs downstream of GSDMD and represses liver regeneration. The discrepancy between those two studies may be due to the different species and strategies used to abolish IL-18. Although GPC3 was up-regulated in liver tumor and promoted the proliferation of hepatoma cells,[38] evidence suggests that it represses normal hepatocyte replication. This discrepancy may be attributed to intrinsic genomic irregularities in hepatoma cells or divergent downstreams of GPC3 between normal and malignancy cells, warranting further investigation. Interestingly, another well-known suppressor of liver regeneration, activin A, was also down-regulated in the regenerating livers of *GSDMD*$^{-/-}$ mice. Activin A belongs to the TGFβ superfamily and signals the same smads as the TGFβ/TβIIR pathway.[39] Compelling evidence has demonstrated that activin A strongly inhibits hepatocyte proliferation and liver regeneration through autocrine signaling.[19,40] Distinct from activin A, while TGFβ induces the growth arrest of hepatocytes *in vitro*,[41] it is not essential for liver regeneration after 70%PH.[40,42] Likewise, the level of TGFβ did not increase after the removal of GSDMD. Our data support that activin A rather than TGFβ is upstream of smad2 phosphorylation. The upstream of activin A was shown to be IL-1β, whose stimulative effect on activin A expression was validated by *in vitro* experiment. It has been shown that IL-1β suppresses liver regeneration after acute liver failure.[35] For liver regeneration after 70%PH, the removal of IL-1Rα, a natural inhibitor of IL-1β that competitively binds to its receptor, also delays liver regeneration.[43] This evidence strongly supports the suppressive role of IL-1β in liver regeneration, and presently, we suggest that the activin A/smad2 axis is downstream of IL-1β in this process. Due to elevated initiation and impaired termination of liver regeneration, the proliferation of hepatocytes and restoration of liver mass were accelerated in *GSDMD*$^{-/-}$ mice compared with controls. Nevertheless, equivalent liver/body weight ratio between GSDMD knockout and wild-type mice 7 days after 70%PH implied that other compensatory pathways were up-regulated to prohibit overgrowth of the liver in *GSDMD*$^{-/-}$ mice.

Pharmacological inhibition of GSDMD by DSF recapitulated the symptom observed in *GSDMD*$^{-/-}$ mice, implying its potential applications in patients with impaired liver regenerative capacity. In liver tumors, DSF was reported to repress tumor metastasis and eradicate tumor initiating cells.[44,45] Our data showed another function of DSF to accelerate liver regeneration. Thus, DSF treatment may benefit patients with liver tumor, not only suppressing hepatoma cells but also promoting normal hepatocytes proliferation. For patients with nonalcoholic steatohepatitis and alcohol-associated hepatitis,[11,24] application of DSF may help to mitigate liver injury and ameliorate liver regeneration by targeting GSDMD-mediated pyroptosis.

In conclusion, the present study demonstrates that caspase-11/GSDMD-mediated pyroptosis negatively regulates liver regeneration after 70%PH. Down-regulated HGF/c-Met and EGFR signaling pathways, and activation of IL-18/GPC3 and the IL-1β/activin A/Smad2 axis, contribute to the biological function of GSDMD in this process. Our results enrich the understanding of the regulatory mechanisms of liver regeneration and supply a potential strategy for improving liver regeneration in patients with liver diseases.

ACKNOWLEDGMENT

We thank Professor Chong Liu from Naval Medical University for kindly providing the *GSDMD*$^{-/-}$ mice.

CONFLICT OF INTEREST

Nothing to report.

AUTHOR CONTRIBUTIONS

Study concept and design: Xiujun Cai, Tong Ji, and Yifan Wang. *Animal and cell experiments:* Xingyu Lv. and Tong Ji *Biochemical and molecular experiments;* Jiang Chen and Jiayan He. *Data analysis:* Tong Ji and Yiyue Ren. *Manuscript draft:* Tong Ji and Xingyu Lv. *Manuscript revisions:* Lidan Hou. and Xiaoyun Shen. All authors read and approved the final version of the manuscript.

REFERENCES

1. Fausto N, Campbell JS, Riehle KJ. Liver regeneration. Hepatology. 2006;43:S45–53.
2. Yanger K, Knigin D, Zong Y, Maggs L, Gu G, Akiyama H, et al. Adult hepatocytes are generated by self-duplication rather than stem cell differentiation. Cell Stem Cell. 2014;15:340–9.
3. Michalopoulos GK, Bhushan B. Liver regeneration: biological and pathological mechanisms and implications. Nat Rev Gastroenterol Hepatol. 2021;18:40–55.

4. Michalopoulos GK. Liver regeneration. J Cell Physiol. 2007;213: 286–300.
5. Shi JH, Line PD. Hallmarks of postoperative liver regeneration: an updated insight on the regulatory mechanisms. J Gastroenterol Hepatol. 2020;35:960–6.
6. Bangru S, Kalsotra A. Cellular and molecular basis of liver regeneration. Semin Cell Dev Biol. 2020;100:74–87.
7. Shi J, Gao W, Shao F. Pyroptosis: gasdermin-mediated programmed necrotic cell death. Trends Biochem Sci. 2017;42: 245–54.
8. Shi J, Zhao Y, Wang K, Shi X, Wang Y, Huang H, et al. Cleavage of GSDMD by inflammatory caspases determines pyroptotic cell death. Nature. 2015;526:660–5.
9. Broz P, Pelegrin P, Shao F. The gasdermins, a protein family executing cell death and inflammation. Nat Rev Immunol. 2020;20:143–57.
10. Liu X, Xia S, Zhang Z, Wu H, Lieberman J. Channelling inflammation: gasdermins in physiology and disease. Nat Rev Drug Discov. 2021;20:384–405.
11. Xu B, Jiang M, Chu Y, Wang W, Chen D, Li X, et al. Gasdermin D plays a key role as a pyroptosis executor of non-alcoholic steatohepatitis in humans and mice. J Hepatol. 2018;68:773–82.
12. Chen R, Zeng L, Zhu S, Liu J, Zeh HJ, Kroemer G, et al. cAMP metabolism controls caspase-11 inflammasome activation and pyroptosis in sepsis. Sci Adv. 2019;5:5562.
13. Miao N, Yin F, Xie H, Wang Y, Xu Y, Shen Y, et al. The cleavage of gasdermin D by caspase-11 promotes tubular epithelial cell pyroptosis and urinary IL-18 excretion in acute kidney injury. Kidney Int. 2019;96:1105–20.
14. Yang C, Sun P, Deng M, Loughran P, Li W, Yi Z, et al. Gasdermin D protects against noninfectious liver injury by regulating apoptosis and necroptosis. Cell Death Dis. 2019;10:481.
15. Ozaki M. Cellular and molecular mechanisms of liver regeneration: proliferation, growth, death and protection of hepatocytes. Semin Cell Dev Biol. 2020;100:62–73.
16. Mitchell C, Willenbring H. A reproducible and well-tolerated method for 2/3 partial hepatectomy in mice. Nat Protoc. 2008;3:1167–70.
17. Li G, Ji T, Chen J, Fu Y, Hou L, Feng Y, et al. CRL4(DCAF8) ubiquitin ligase targets histone H3K79 and promotes H3K9 methylation in the liver. Cell Rep. 2017;18:1499–511.
18. Ma T, Zhang Y, Lao M, Chen W, Hu Q, Zhi X, et al. Endogenous interleukin 18 suppresses liver regeneration after hepatectomy in mice. Liver Transpl. 2020;26:408–18.
19. Haridoss S, Yovchev MI, Schweizer H, Megherhi S, Beecher M, Locker J, et al. Activin A is a prominent autocrine regulator of hepatocyte growth arrest. Hepatol Commun. 2017;1:852–70.
20. Arai KY, Ono M, Kudo C, Fujioka A, Okamura R, Nomura Y, et al. IL-1beta stimulates activin betaA mRNA expression in human skin fibroblasts through the MAPK pathways, the nuclear factor-kappaB pathway, and prostaglandin E2. Endocrinology. 2011;152:3779–90.
21. Hu JJ, Liu X, Xia S, Zhang Z, Zhang Y, Zhao J, et al. FDA-approved disulfiram inhibits pyroptosis by blocking gasdermin D pore formation. Nat Immunol. 2020;21:736–45.
22. Ozaki M, Haga S, Ozawa T. In vivo monitoring of liver damage using caspase-3 probe. Theranostics. 2012;2:207–14.
23. Xia S, Hollingsworth LRT, Wu H. Mechanism and regulation of gasdermin-mediated cell death. Cold Spring Harb Perspect Biol. 2020;12:a036400.
24. Khanova E, Wu R, Wang W, Yan R, Chen Y, French SW, et al. Pyroptosis by caspase11/4-gasdermin-D pathway in alcoholic hepatitis in mice and patients. Hepatology. 2018;67:1737–53.
25. Arechederra M, Berasain C, Avila MA, Fernandez-Barrena MG. Chromatin dynamics during liver regeneration. Semin Cell Dev Biol. 2020;97:38–46.
26. Tao Y, Wang M, Chen E, Tang H. Liver regeneration: analysis of the main relevant signaling molecules. Mediators Inflamm. 2017;2017:4256352.
27. Natarajan A, Wagner B, Sibilia M. The EGF receptor is required for efficient liver regeneration. Proc Natl Acad Sci U S A. 2007;104:17081–6.
28. Zarnegar R, DeFrances MC, Kost DP, Lindroos P, Michalopoulos GK. Expression of hepatocyte growth factor mRNA in regenerating rat liver after partial hepatectomy. Biochem Biophys Res Commun. 1991;177:559–65.
29. Paranjpe S, Bowen WC, Mars WM, Orr A, Haynes MM, DeFrances MC, et al. Combined systemic elimination of MET and epidermal growth factor receptor signaling completely abolishes liver regeneration and leads to liver decompensation. Hepatology. 2016;64:1711–24.
30. Berasain C, Garcia-Trevijano ER, Castillo J, Erroba E, Lee DC, Prieto J, et al. Amphiregulin: an early trigger of liver regeneration in mice. Gastroenterology. 2005;128:424–32.
31. Michalopoulos GK. Advances in liver regeneration. Expert Rev Gastroenterol Hepatol. 2014;8:897–907.
32. Robinson N, Ganesan R, Hegedus C, Kovacs K, Kufer TA, Virag L. Programmed necrotic cell death of macrophages: focus on pyroptosis, necroptosis, and parthanatos. Redox Biol. 2019;26:101239.
33. Seki E, Kondo Y, Iimuro Y, Naka T, Son G, Kishimoto T, et al. Demonstration of cooperative contribution of MET- and EGFR-mediated STAT3 phosphorylation to liver regeneration by exogenous suppressor of cytokine signalings. J Hepatol. 2008;48:237–45.
34. Yu P, Zhang X, Liu N, Tang L, Peng C, Chen X. Pyroptosis: mechanisms and diseases. Signal Transduct Target Ther. 2021;6:128.
35. Tan Q, Hu J, Yu X, Guan W, Lu H, Yu Y, et al. The role of IL-1 family members and kupffer cells in liver regeneration. Biomed Res Int. 2016;2016:6495793.
36. Zhang J, Ma C, Liu Y, Yang G, Jiang Y, Xu C. Interleukin 18 accelerates the hepatic cell proliferation in rat liver regeneration after partial hepatectomy. Gene. 2014;537:230–7.
37. Liu B, Bell AW, Paranjpe S, Bowen WC, Khillan JS, Luo JH, et al. Suppression of liver regeneration and hepatocyte proliferation in hepatocyte-targeted glypican 3 transgenic mice. Hepatology. 2010;52:1060–7.
38. Nishida T, Kataoka H. Glypican 3-targeted therapy in hepatocellular carcinoma. Cancers (Basel). 2019;11:1339.
39. Chen YG, Wang Q, Lin SL, Chang CD, Chuang J, Ying SY. Activin signaling and its role in regulation of cell proliferation, apoptosis, and carcinogenesis. Exp Biol Med (Maywood). 2006;231:534–44.
40. Oe S, Lemmer ER, Conner EA, Factor VM, Leveen P, Larsson J, et al. Intact signaling by transforming growth factor beta is not required for termination of liver regeneration in mice. Hepatology. 2004;40:1098–105.
41. Houck KA, Michalopoulos GK. Altered responses of regenerating hepatocytes to norepinephrine and transforming growth factor type beta. J Cell Physiol. 1989;141:503–9.
42. Sanderson N, Factor V, Nagy P, Kopp J, Kondaiah P, Wakefield L, et al. Hepatic expression of mature transforming growth factor beta 1 in transgenic mice results in multiple tissue lesions. Proc Natl Acad Sci U S A. 1995;92:2572–6.
43. Sgroi A, Gonelle-Gispert C, Morel P, Baertschiger RM, Niclauss N, Mentha G, et al. Interleukin-1 receptor antagonist modulates the early phase of liver regeneration after partial hepatectomy in mice. PLoS One. 2011;6:e25442.
44. Chiba T, Suzuki E, Yuki K, Zen Y, Oshima M, Miyagi S, et al. Disulfiram eradicates tumor-initiating hepatocellular carcinoma cells in ROS-p38 MAPK pathway-dependent and -independent manners. PLoS One. 2014;9:e84807.

45. Li Y, Wang LH, Zhang HT, Wang YT, Liu S, Zhou WL, et al. Disulfiram combined with copper inhibits metastasis and epithelial-mesenchymal transition in hepatocellular carcinoma through the NF-kappaB and TGF-beta pathways. J Cell Mol Med. 2018;22:439–51.

SUPPORTING INFORMATION

Additional supporting information may be found in the online version of the article at the publisher's website.

How to cite this article: Lv X, Chen J, He J, Hou L, Ren Y, Shen X, Gasdermin D–mediated pyroptosis suppresses liver regeneration after 70% partial hepatectomy. Hepatol Commun. 2022;6:2340–2353. https://doi.org/10.1002/hep4.1973